DOI: 10.1007/s11099-018-0824-6 PHOTOSYNTHETICA 56 (4): 998-1009, 2018

Transcriptome profiling of genes involved in photosynthesis in *Elaeagnus angustifolia* L. under salt stress

J. LIN[#], J.P. LI[#], F. YUAN, Z. YANG, B.S. WANG[+], and M. CHEN[+]

Shandong Provincial Key Laboratory of Plant Stress Research, College of Life Science, Shandong Normal University, Shandong 250014, China

Abstract

High salt concentration is a major abiotic stress limiting plant growth and productivity in many areas of the world. *Elaeagnus angustifolia* L. adapts to adverse environments and is widely planted in the western region of China as a windbreaker and for landscape and soil stabilization. High salt concentrations inhibited photosynthesis of *E. angustifolia*, but the mechanism is not known. In this paper, RNA-sequencing was used to investigate effects of salt stress on the photosynthetic characteristics of the species. In total, 584 genes were identified and involved in photosynthetic pathways. The downregulation of genes that encode key enzymes involved in photosynthesis and genes correlated to important structures in photosystem and light-harvesting complexes might be the main reason, particularly, the downregulation of the gene that encodes magnesium chelatase. This would decrease the activity of enzymes involved in chlorophyll synthesis and the downregulation of the key gene that encodes Rubisco, and thereby decreases enzyme activity and the protein content of Rubisco.

Additional key words: biomass; greening; ion concentrations; photosynthetic parameters; plant height.

Introduction

Global soil salinization is becoming increasingly serious problem (Zhu 2001). Among 230 million hectares of irrigated farm land, 20% are affected by salt, and the proportion is increasing every year as a result of unsuitable irrigation practices (Deinlein *et al*. 2014). China contains approximately 100 million ha of saline soils, and in the Yellow River Delta of China alone, the area of saline land is expanding at a rate of $1.3 \times 10^3 – 2.0 \times 10^3$ ha per year. Thus, soil salinity has become a major environmental factor limiting plant growth by impacting plant height, biomass, and ion contents, among other parameters. Salt stress involves a combination of osmotic and ionic stress that greatly affects plant growth and crop production. The saline soil of the Yellow River Delta is not suitable for the growth of crops and young forests because of its high salt content, high underground water level, and deficiency of organic matter, nitrogen and phosphorus. These unfavorable factors have slowed urban road greening around the

Received 27 June 2017, *accepted* 22 November 2017, *published as online-first* 17 April 2018.
[+]Corresponding authors; phone: +86 531 86180197, fax: +86 531 86180107, e-mail: bswang@sdnu.edu.cn; chenminrundong@126.com
Abbreviations: CDS – predicted conding sequence; C_i – intercellular CO_2 concentration; COG – clusters of orthologous groups; DEG – differentially expressed gene; DM – dry mass; *E* – transpiration rate; FDR – false discovery rate; FM – fresh mass; FPKM – fragments per kilobase of exon model; F_v/F_m – maximum photochemical efficiency of PSII; g_s – stomatal conductance; PEPC – phospho*enol*pyruvate carboxylase; P_N – net photosynthetic rate; PPDK – pyruvate orthophosphate dikinase; RNA-Seq – RNA-sequencing; RPKM – reads per KB per million; SNP – simple nucleotide polymorphism; SSR – simple sequence repeat; Φ_{PSII} – actual PSII efficiency.
Acknowledgements: This work was supported by the National Natural Science Foundation of China (Grant 31400239, 31600200), the National Basic Research Program of China (Grant 2012CB114201), the Science and Technology Development Projects of Shandong Province (Grant 2013GNC11310), Independent Innovation and Achievement Transformation of Special Major Key Technical Plans of Shandong Province (2017CXGC0311), and the Program for Scientific Research Innovation Team in Colleges and Universities of Shandong Province.
[#]These authors contributed equally to this work.

Yellow River Delta; therefore, saline soil is substituted with normal soil for greening. Since the costs of soil replacement and greening maintenance programs are high, the decreasing proportion of forestation results in woodland shortages. Thus, it is important to explore the physiological and molecular mechanisms involved in plant responses to salt stress in order to implement measures for reduction of salt damage to plants. *Elaeagnus angustifolia* [L.] (Russian olive, also known as oleaster), which grows as a deciduous shrub or small tree, is a member of the Elaeagnaceae family. Leaves of the species are simple, alternate, and lanceolate to oblong, and are entire along the leaf margins (Amezketa 2006). The growth period of the species is from April to October because it is resistant to cold. Its flowers are attractive, colorful, diverse, and aromatic; hence, it is also known as aromatic willow and silvery bud willow (Amezketa 2006). The species exhibits a high fruit yield; the fruits are rich in sugar and can therefore be used as feed, fuel, timber, and medicine. Being resistant to drought, salinity, and infertility, *E. angustifolia* is widely planted in the western region of China as a windbreaker and for landscape and soil stabilization. As an uncommon type of halophytic energy plant, the species produces abundant biomass from saline resources (Ahmadiani *et al*. 2000). It is important to fully understand the mechanism of salt tolerance of the species and introduce it as a green tree in the Yellow River Delta. Munns and Tester (2008) showed that the photosynthetic rate, assimilation, and energy supply are all reduced under salt stress, thereby limiting the growth and development of plants. Photosynthesis plays an important role in *E. angustifolia* seedling growth under salt stress, but the underlying molecular mechanisms remain largely unknown. The photosynthetic capacity of seedlings of the species significantly decreased under Na_2SO_4 treatment (Liu *et al*. 2014). It has been reported that the photosynthetic capacity of seedlings of the species declined under a low salt concentration (≤ 200 mM Na_2SO_4), mainly due to stomatal factors; however, the photosynthetic capacity is also affected by a high salt concentration (300 mM Na_2SO_4), mainly due to nonstomatal factors (Liu *et al*. 2005). The growth and physiology of the species are directly inhibited by NaCl treatment, ultimately causing a decrease in plant biomass (Liu *et al*. 2014).

Upon a salt treatment, many major physiological processes are disturbed, such as photosynthesis, protein synthesis, energy metabolism, and lipid metabolism. Thus, the expression of some genes involved in the above processes is also assumed to be regulated by salt. In recent years, with the increasing amount of available sequence data, expression profiling has been used to identify genes involved in adaptive responses to abiotic stresses. A common strategy for identifying genes related to salt stress is comparative analysis of different genotypes or cultivars that are tolerant to abiotic stress (Kalaitzis *et al*. 2012). Transcriptome data for genes that are differentially expressed (DEG, differentially expressed gene) in *Halostachys caspica* under salt stress (600 mM NaCl) have been analyzed using bioinformatics methods. The changes in the expression of transcription-factor genes in two melon (*Cucumis melo* L.) cultivars (Yvlu and Bingxuecui) under salt stress have been analyzed using RNA-sequencing (Seq) next-generation high-throughput sequencing technology. Chlorophyll (Chl) fluorescence parameters were found to differ between these two cultivars, indicating significant differences in their salt tolerance. The results revealed 56 differentially expressed transcription factor genes belonging to 19 transcription factor families in YvLu and 47 transcription factor genes belonging to 20 transcription factor families in Bingxuecui under salt stress (Chen *et al*. 2014). We can better understand the salt tolerance mechanism of *E. angustifolia* at the molecular level through transcriptome analysis. A total of 3,008 DEGs were identified between the species control seedlings and those subjected to salt stress. This study provides further insight into the complex regulatory pathways underlying the mechanism of photosynthesis under salt stress in the species.

Materials and methods

Plant materials and growth conditions: Seeds of *E. angustifolia* collected from the Shiyanghe region of Gansu province, China, were used as the experimental materials in this study. Uniform seeds were selected and sown in plastic pots (16 × 21 cm) filled with river sand, which was rinsed repeatedly until water used for rinsing ran clear; they were irrigated with water. The seedlings were established from germination to the first true-leaf stage and were cultured at 24 ± 3°C (16-h light, 8-h dark) in glasshouse under a light intensity of 600 μmol(photon) m^{-2} s^{-1} and relative humidity of 70%. After germination, the seedlings were irrigated with 1/2 Hoagland solution. Salt treatment was performed at the four-leaf stage. The treated plants were irrigated with Hoagland nutrient solution containing 0, 75, 150, 225, or 300 mM NaCl. The NaCl concentration was increased stepwise towards the final concentrations in increments of 75 mM per day.

Plant height, mass and inorganic ions: After exposure to the salt treatment for 7 d, 20 plants from each treatment were used to determine plant height. After washing the plant samples, the fresh mass (FM) and dry mass (DM) of the shoots and roots, the contents of inorganic ions of the expanding leaves, expanded leaves and roots were measured separately according to the methods described by Song (2006).

Chl fluorescence: After exposure to salt treatment for 7 d, Chl fluorescence parameters were measured independently in 15 plants per treatment. Measurements were performed on the mature leaves of each plant using a portable fluorometer (*FMS2*, *Hansatech*, King's Lynn, UK) following the protocol described by Kooten and Snel (1990). The leaves were pre-darkened for 30 min. Maximal fluorescence (F_m) was determined using 0.8-s saturating light of 8,000 μmol(photon) m^{-2} s^{-1}. Then, the leaf was illuminated by actinic light of 500 μmol(photon) m^{-2} s^{-1}. Steady-state fluorescence (F_s) was recorded when the leaf reached steady-state photosynthesis. The second flash of 0.8-s saturating light of 8,000 μmol(photon) m^{-2} s^{-1} was provided to determine maximal fluorescence in the light-adapted state (F_m'). The maximal photochemical efficiency (F_v/F_m) of PSII was expressed as $F_v/F_m = (F_m - F_0)/F_m$. The actual quantum yield of PSII was expressed as $\Phi_{PSII} = (F_m' - F_s)/F_m'$.

Chl content: After exposure to the salt treatment for 7 d, leaves (0.2 g FM) were washed in distilled water and then put into the extract solution to extract Chl according to the methods described by Sui (2015). The absorbance of the extract was determined at 663 and 645 nm using a *BECKMAN DU2600* spectrophotometer (*Puxi Biological Technology Co*., Beijing, China). The amount of total Chl was calculated using the Arnon (1949) formulas.

Photosynthesis: After exposure to the salt treatment for 7 d, net photosynthetic rate (P_N), stomatal conductance (g_s), and intercellular CO_2 concentration (C_i) were measured using an *Li-6400* photosynthesis measurement system (*LI-COR, Inc*., Lincoln, NE, USA). The measurements were performed outdoors from 10:00 to 12:00 h on the mature leaves of each of the chosen plants (15 replicates per treatment).

Protein content and activity of magnesium chelatase and Rubisco: Magnesium chelatase and Rubisco were prepared by first freezing a 0.2-g leaf sample in liquid nitrogen to prevent proteolytic activity, followed by grinding with 2 mL of extraction buffer (100 mM phosphate buffer, pH 7.2, containing 0.1 mM EDTA, and 2 mM ascorbic acid). The homogenate was centrifuged for 15 min at 10,000 rpm, and the supernatant was used to measure the protein content (ng L^{-1}), magnesium chelatase activity [pmol(Mg-Deutero) min^{-1} mg^{-1}(protein)] and Rubisco activity [μmol min^{-1} mg^{-1}(protein)]. Magnesium chelatase and Rubisco were measured using a magnesium chelatase content kit and a Rubisco content kit (double antibody sandwich method, *Huding Biological Technology Co*., Shanghai, China) (3 replicates per treatment).

RNA-Seq analysis: Total RNA was extracted from the leaves of *E. angustifolia* seedlings treated with 0 or 150 mM NaCl for 48 h using the *Total Plant RNA Extraction Kit* (*Karroten*, Beijing, China) following the manufacturer's protocol. For each biological replicate, 15 plants were used for RNA isolation, with two to three leaves being collected from each plant. Leaf tissue samples of 0.2 g were used for isolation. The plants used for RNA isolation were independently grown and treated. RNA was quantified using a *NanoDrop ND-1000* spectrophotometer (*Thermo Fisher Scientific*, Wilmington, DE, USA). The integrity of the RNA was determined in a 1% agarose gel buffered by Tris–acetate–EDTA. mRNA was randomly fragmented with a fragmentation buffer. Using the mRNA as a template, the first strand of cDNA was synthesized with six-base random primers (random hexamers), after which the buffer solution, dNTPs, RNase H, and DNA polymerase I were added to synthesize the second strand of cDNA. The cDNA was purified using *AMPure XP* beads. The double-stranded cDNA was then purified; the distal ends were repaired; a tail and sequencing adapters were connected; and *AMPure XP* beads were used for fragment size selection. Finally, a cDNA library was obtained *via* PCR enrichment. After the completion of library construction, the size of the library and the insert sizes were detected using *Qubit 2.0* and an *Agilent 2100* system (*BioMarker Technologies Co. Ltd.*, Beijing, China), respectively. In addition, to ensure the quality of the library, qPCR was used for accurate quantification of the effective library size. The final cDNA library was sequenced using the *Illumina Hi-Seq™ 2500* platform at *BioMarker Technologies Co. Ltd.*, Beijing. RNA-Seq data for the untreated control and salt-treated samples were obtained from two biological replicates. In order to generate clean reads, the raw reads were cleaned by removing adapter sequences, empty reads, and low-quality sequences.

Gene annotation and classifications were carried out according to Sui (2015) and the assembled sequences were compared against the *National Center for Biotechnology Information* (NCBI) nonredundant (nr) database, *Swiss-Prot*, *Gene Ontology* (GO) analysis (Ashburner *et al*. 2000; Sun *et al*. 2010), the *Clusters of Orthologous Groups*

(COG) classification (Bazakos *et al*. 2012), and the Kyoto Encyclopedia of Genes and Genomes (KEGG) (Kanehisa *et al*. 2004) database using *BLAST* with E-value ≦ 1 e^{-10} as the cutoff (Sui *et al*. 2015).

Data analysis: Libraries were constructed following a high-throughput *Illumina* strand-specific RNA sequencing library protocol. Clean reads were mapped to the species genome using *TopHat* version *2.1.10*. Reads per KB per million (RPKM) values were calculated with an in-house script according to the number of bases. The RPKM measure of read density reflects the molar concentration of a transcript in the starting sample based on normalization for RNA length and for the total read number in the measurement. An RPKM threshold value of 0.1 was set to detect the presence of a transcript for a particular gene. DEGs were defined using DESeq as those showing fold changes ≥ 2 with a false discovery rate (FDR) adjusted *P*-value≤0.01.

The assembled sequences were compared against the NCBI non-redundant (nr) database as well as the *Swiss-Prot*, GO, COG, and KEGG databases using *BLAST*, with an E-value ≤ l e^{-10} as the cutoff (Conesa *et al.* 2005).

To examine the functional changes in *E. angustifolia* leaves under salt stress, DEGs were identified by applying DESeq. The enriched GO terms for each cluster were analyzed using *Fisher*'s test with an FDR ≤ 0.01 employing an in-house PERL script. For the calculation of gene expression, a fragments per kilobase of exon model (FPKM) was employed. For example, a total of 61 genes were annotated to the mitochondria. Under salt stress, the FPKM values of nine genes were less than 1, and these genes were expressed only in the control group. In the control group, only one gene exhibited an FPKM value of less than 1; this gene was expressed only under salt stress.

Quantitative real-time PCR analysis: To validate the accuracy of the RNA-Seq results, 18 DEGs were randomly selected to perform quantitative real-time PCR. Most of these genes were related to photosynthesis. Primers for these 18 genes were designed using *Primer 5.0*. The β-actin housekeeping gene of the species (GenBank ID: X79378) was used as an internal standard. One microgram of total RNA was employed for each 20-μL reaction for reverse transcription. PCR was performed in a 20-μL reaction mixture with 6.5 μL of double-distilled H_2O, 0.5 μL of both the forward and reverse primers, 2.5 μL (20 ng μL^{-1}) of cDNA, and 10 μL of *SYBR Premix Ex Taq* (*Bio-Rad*, California, USA). Real-time PCR was performed on a real-time quantitative PCR instrument (*Bio-Rad*, California, USA). The 2-ΔΔCt method was used to calculate the relative expression of each gene (Livak and Schmittgen 2001).

Statistical analysis: Multiple comparisons were performed between different samples using *Duncan's* test at the 0.05 significance level (Khavarinejad and Mostofi 1998). All tests were performed with *SPSS Version 17.0* for *Windows* (*SPSS*, Chicago. IL, USA).

Availability of data and materials: The data sets supporting the results of this article are included within the article and its additional files. The reads produced in this study have been deposited in the NCBI SRA database with accession number of SRS1876111 for control, SRS1876112 for salt-treated. Access to the data is available upon publication at https://www.ncbi.nlm.nih.gov/bioproject/?term=PRJ NA357541.

Results

Plant height and biomass: The effect of NaCl on plant height was the same as that on seedling biomass (Fig. 1*A–C*). A low NaCl concentration (75 mM) had no effect on plant height, shoot fresh mass (FM), and dry mass (DM), but plant height, shoot FM and DM decreased significantly with an increasing NaCl concentration. The higher the concentration of NaCl, the more obvious decline in the plant height, shoot FM and DM.

Ion concentrations: With an increasing NaCl concentration, the Na^+ contents of the leaves (including expanding and expanded leaves) and roots increased significantly (Fig. 2*A*). Under the NaCl treatment, the Na^+ content of the roots exhibited the most significant increase, followed by that of expanded leaves. Under the treatment with same concentration of NaCl, the Na^+ concentration in the roots was the highest, followed by that in the expanded leaves, while the Na^+ concentration in the expanding leaves was the lowest one.

With an increasing NaCl concentration, the K^+ contents in the leaves (including expanding and expanded leaves) and roots decreased significantly (Fig. 2*B*). Under NaCl treatment, the K^+ contents of the roots exhibited the most significant decrease. Moreover, under the treatment with

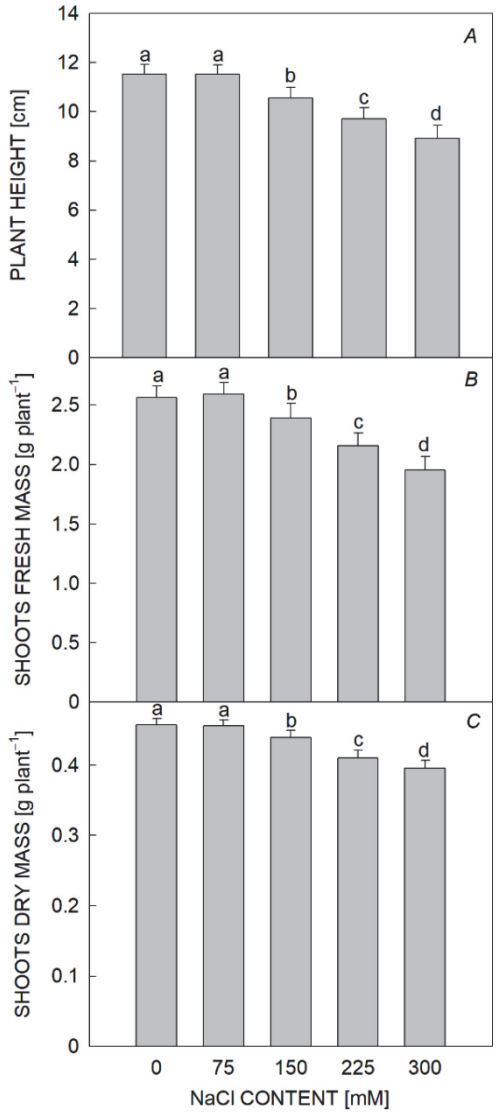

Fig. 1. Effects of NaCl on the plant height (*A*), shoots fresh mass (*B*), and dry mass (*C*) of *Elaeagnus angustifolia* seedlings. Values are means ± SD of 20 replicates for each of 20 plants. Bars with the *different letters* are significantly different at $P<0.05$ according to *Duncan*'s multiple range tests.

the same concentration of NaCl, the K^+ content in the roots was the lowest, followed by the expanded leaves and, finally, by the expanding leaves.

Chl content of *E. angustifolia* leaves was quantified after 7 d of exposure to NaCl. There was no significant difference in the content of Chl between the 75 mM NaCl-treated leaves and the non-treated leaves. However, the Chl *a*, Chl *b*, and total Chl contents all decreased dramatically under increasing NaCl concentrations (150, 225, and 300 mM) (Fig. 3).

Actual PSII quantum efficiency: The maximal efficiency of PSII photochemistry (F_v/F_m) was reduced with the increasing NaCl concentration (Fig. 4*E*). The F_v/F_m of leaves under 75 mM NaCl treatment was similar to that without the NaCl treatment. After treatment with 150, 225, and 300 mM NaCl, F_v/F_m decreased significantly.

The actual efficiency of PSII (Φ_{PSII}) in the leaves showed a similar trend to F_v/F_m (Fig. 4*F*). Leaf Φ_{PSII} remained unchanged under the treatment with 75 mM NaCl, but decreased with higher NaCl concentrations (150–300 mM NaCl).

Photosynthetic parameters: With an increasing NaCl concentration, the P_N, g_s. and transpiration rate (E) showed similar trends (Fig. 4). Interestingly, the values of P_N, g_s, and E under the treatment with 75 mM NaCl were significantly higher than those of the control, whereas the values under 150–300 mM NaCl treatment were lower (in the same descending gradient order) than those of the controls under the same conditions. In addition, the C_i gradually decreased, corresponding to the descending gradient of NaCl concentrations.

Quality of RNA-Seq data: To investigate the molecular mechanisms underlying photosynthesis in the species seedlings under salt stress, RNA-Seq libraries were designed using mRNA extracted from the species seedlings treated with 0 mM or 150 mM NaCl for 48 h. After filtering low-quality reads and trimming adapters, 38.52 gigabases (Gb) of clean reads were retained for assembly and further analysis. In the sequencing data for the samples to 4G, the Q30 base percentage was greater than 90.63%. *De novo* assembly resulted in a total of 121,488 uni-genes, 19,268 of which were longer than 1 kilobase (kb). Based on the genetic structure of the unigene database analysis, including the analysis of predicted coding sequences (CDSs), simple sequence repeats (SSRs), and sample simple nucleotide polymorphisms (SNPs), a total of 10,840 SSR markers were obtained. All of these data showed that the throughput and sequencing quality were sufficiently high for further analysis.

Systematic analysis of the data of RNA-sequence: The uni-genes were assembled in the species with 83,638 genes in the control and 82,961 in the NaCl-treated plants. In total, 69,620 common genes were found between the control and NaCl-treated plants, and 13,341 genes showed specific expression under the NaCl treatment (Fig. 5) which means that these genes may play an essential role in salt resistance of *E. angustifolia* plants. Different expression patterns of DE genes were observed by cluster analysis (Fig. 1S, *supplement available online*).

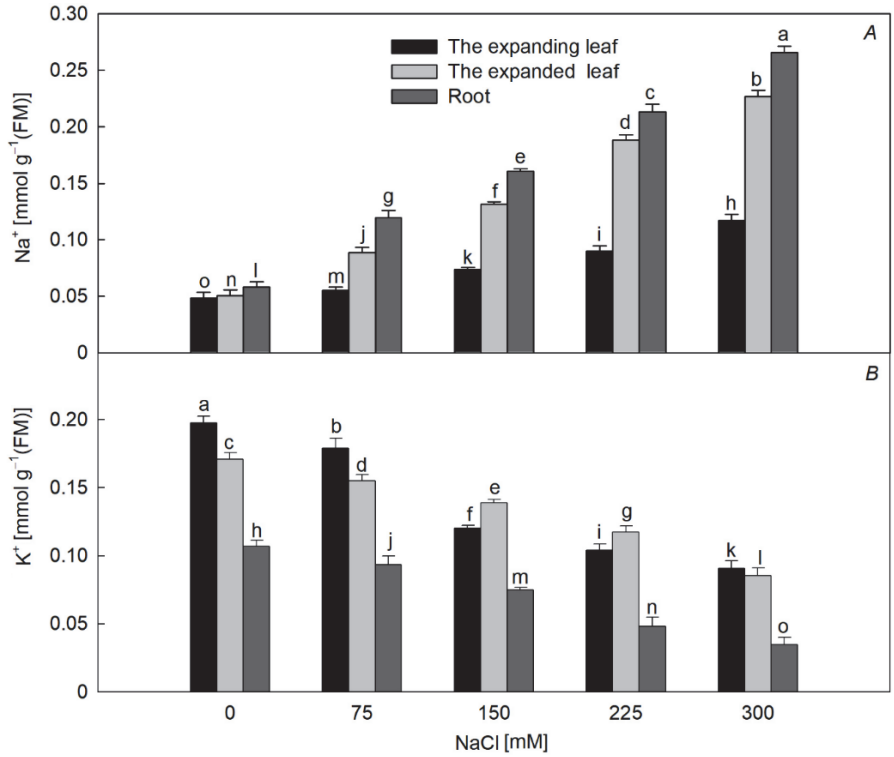

Fig. 2. Effect of NaCl on ion contents of *Elaeagnus angustifolia* seedlings. Values are means ± SD of three replicates. Bars with the *different letters* are significantly different at $P<0.05$ according to *Duncan*'s multiple range tests.

Functional classification of differentially expressed genes by GO, COG, and KEGG annotation: To assign functional information to the DEGs between the control and NaCl-treated plants, GO analysis was carried out. This type of analysis assigns functional information to DEGs. A total of 1,754 unique transcripts were assigned to 48 level-2 GO terms, in three main GO categories, including 16 for cellular components (CC), 16 for molecular functions (MF), and 20 for biological processes (BP) (Fig. 4S, *supplement available online*).

The COG analysis assigned functional information to the DEGs identified between control plants and those treated with NaCl. Among the 25 COG categories, the "general function prediction only" group was the largest one, followed by the "transcription", "signal transduction mechanisms", "lipid transport and metabolism", "amino acid transport and metabolism", and "carbohydrate transport and metabolism" groups (Fig. 2S, *supplement available online*). There were few corresponding genes in the groups of "chromatin structure and dynamics" and "cell motility". No corresponding genes were found in the "extracellular structures" or "nuclear structure" groups.

In total, 582 DEGs were assigned to 50 KEGG pathways. Some of these DEGs mapped to "photosynthesis", "photosynthesis-antenna proteins", and "chlorophyll metabolism", which indicated that NaCl stress affects photosynthesis (Fig. 3S and Table 1S, *supplements available online*).

Exploration of DEGs in response to NaCl: In the presence of salt, we identified 3,008 DEGs in *E. angustifolia* seedlings using the DEseq method. According to the annotation of differentially expressed genes from the GO database, we found that 754 of the 3,008 DEGs were related to the NaCl responses of the species. Among these functions, the difference in the number of expressed genes between the NaCl stress and control groups was significant, indicating that NaCl stress had a greater impact on these functions (Fig. 1S). Among the 754 genes, 202 were associated with the chloroplast, 167 genes with transferase activity, 61 genes with the mitochondria, 40 genes with ATPase activity, 27 genes with calcium, 36 genes with abscisic acid, 25 genes with auxin, 25 genes with plasmodesmata, and 30 genes were associated with photosynthesis (Fig. 6).

Chl metabolism and photosynthetic-antenna proteins: In the present study, 7 DEGs of *E. angustifolia* seedlings

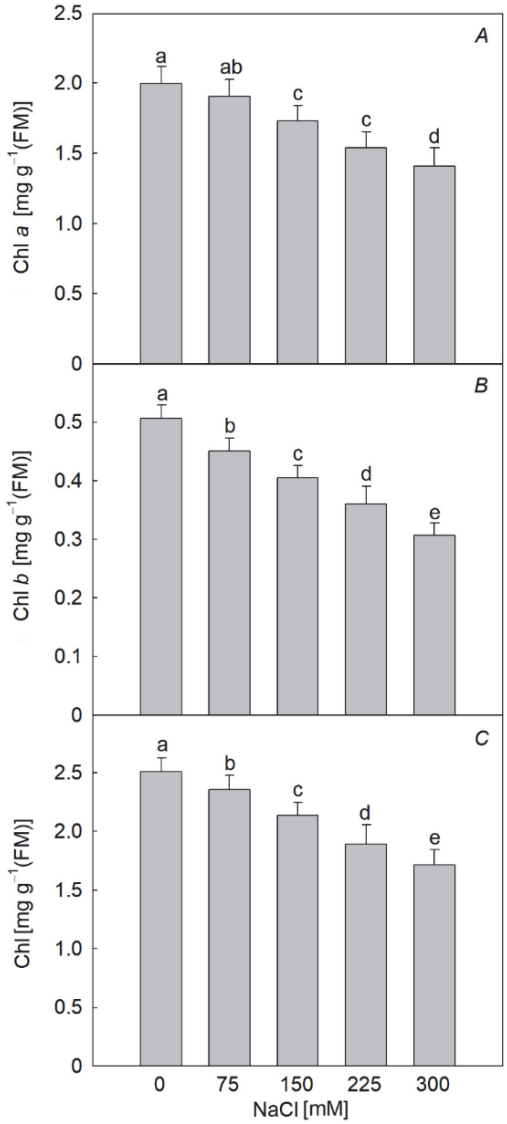

Fig. 3. Effect of NaCl on the chlorophyll content of *Elaeagnus angustifolia* seedlings leaves. Values are means ± SD of 15 replicates. Bars with the *different letters* are significantly different at $P<0.05$ according to *Duncan*'s multiple range tests.

were mapped to the pathway of Chl metabolism (Fig. 5S, *supplement available online*). After the treatment with NaCl, the expression of DEGs encoding protoporphyrinogen oxidase, magnesium chelatase subunit chlD, magnesium chelatase subunit chlI, protochlorophyllide reductase A, and protochlorophyllide reductase C was downregulated.

In the present study, 8 DEGs of *E. angustifolia* seedlings were mapped to antenna proteins. In comparison with the untreated control, the expression of the DEGs encoding *Lhca*3, *Lhcb*1, *Lhcb*3, *Lhcb*4, and *Lhcb*6 was downregulated under NaCl stress (Fig. 6S, *supplement available online*).

Protein content and activity of magnesium chelatase: The activity of magnesium chelatase in the leaves of the species seedlings was markedly ihibited by 150 mM NaCl treatment, although its protein content did not change (Fig. 7*A*). Under 150 mM NaCl treatment, the activity of magnesium chelatase was only 65.4% of that in the control.

Photosynthesis and genes encoding PSII and PSI: In the seedlings, 8 DEGs mapped to the photosynthetic pathway. In comparison with the control, 4 DEGs were downregulated, and 4 DEGs were upregulated under NaCl stress. The DEGs may lead to changes in the structure and function of the four protein components.

Carbon fixation in photosynthetic organs: A total of 9 DEGs in the species mapped to the carbon fixation in photosynthetic organs pathway. Rubisco, phospho*enol*-pyruvate carboxylase (PEPC), and pyruvate orthophosphate dikinase (PPDK) are considered key enzymes in the process of carbon fixation (Whitney *et al*. 2011). The expression levels of *PPDK* and *PEPC* remained unchanged under salt stress according to our RNA-Seq data. The expression of one DEG encoding Rubisco decreased, while another DEG encoding Rubisco increased markedly after 48 h of salt stress. Rubisco is important because it catalyzes the incorporation of CO_2 into ribulose-1,5-bisphosphate. The expression of DEGs encoding fructose-1,6-bisphosphatase, triosephosphate isomerase, malate dehydrogenase, and ribose-5-phosphate isomerase decreased under salt stress.

Protein content and activity of Rubisco: The activity and protein content of Rubisco in the leaves of *E. angustifolia* seedlings were markedly inhibited by 150 mM NaCl treatment (Fig. 7*B*). Under this treatment, the activity and protein content of Rubisco were only 61.5 and 70.4%, respectively, of those in the control.

Verification of RNA-Seq data *via* real-time PCR: In quantitative real-time PCR (qPCR), the accumulation of amplification products is detected using a dual-labeled fluorogenic probe. qPCR provides accurate and reproducible quantitation of gene copies (Heid *et al*. 1996). The method presents a large dynamic range of determination of starting target molecules. We performed q-PCR on 18 randomly selected DEGs to validate the RNA-Seq gene expression analysis. The results obtained through q-PCR showed the same differences in the expression of the 18 genes expressed under NaCl treatment as observed in the

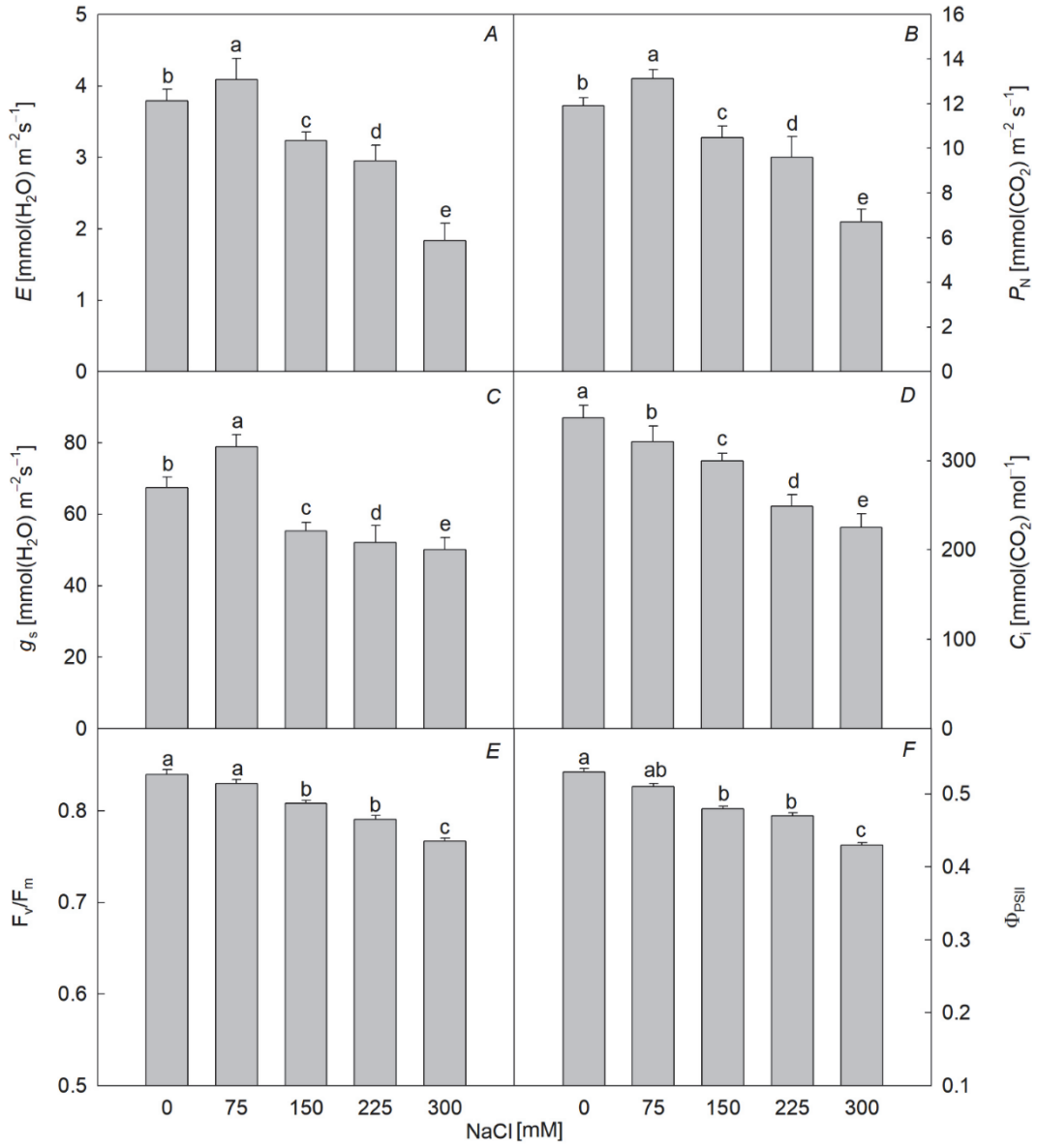

Fig. 4. Effects of NaCl on transpiration rate (*E*, *A*), net photosynthetic rate (P_N, *B*), stomatal conductance (g_s ,*C*), intercellular CO_2 concentration (C_i, *D*), maximal quantum yield of PSII photochemistry (F_v/F_m, *E*), and effective quantum yield of PSII photochemistry (Φ_{PSII}, *F*) of *Elaeagnus angustifolia* seedlings leaves. Values are means ± SD of 15 replicates for each of 15 plants. Bars with the *different letters* are significantly different at $P<0.05$ according to *Duncan*'s multiple range tests.

RNA-Seq gene expression analysis, indicating that the information from the RNA-Seq gene expression analysis was highly reliable (Fig. 8). In addition, the identification of 8 genes that may play important roles in photosynthesis in *E. angustifolia* seedlings was confirmed by q-PCR.

Discussion

Salt stress can disrupt the normal growth of plants (Khodarahmpour 2011). Biomass is the most obvious indicator reflecting the status of plant growth (Pagano and Maddonni 2007). It is well established that plants suffering from salt stress exhibit lower growth rates, smaller leaves, and shorter stems (Curtis and Lanchli 1986, Alshammary

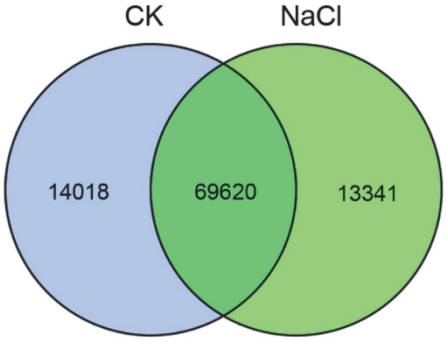

Fig. 5. The commonly and uniquely expressed genes under the control and NaCl treatment of *Elaeagnus angustifolia* seedlings. The genes were showed by the Venn diagram [expression threshold fragments per kilobase of exon model (FPKM) ≥ 1.0].

et al. 2004). Our results showed obvious declines in plant height and biomass with increasing salt concentrations (Fig. 1). Under salt stress, plants suffer from ionic and osmotic stress. Salt-tolerant plants subjected to salt stress can accumulate high concentrations of inorganic ions to in order to lower the osmotic potential in response to salinity, which enables them to absorb water from saline soils, ensuring continued growth (Zhao *et al*. 2003). Under a high concentration of salt, Na^+ can compete with K^+ for ion-binding sites in the plasma membrane, disrupting Na^+/K^+ homeostasis (Feki *et al*. 2014, Kerkeb *et al*. 2001) and damaging plants. Under a treatment with low concentrations of salt, the roots could effectively prevent Na^+ accumulation in the underground parts of plants, protecting the shoots from ionic stress. However, under high salt concentrations, the capacity of the roots was exceeded, and

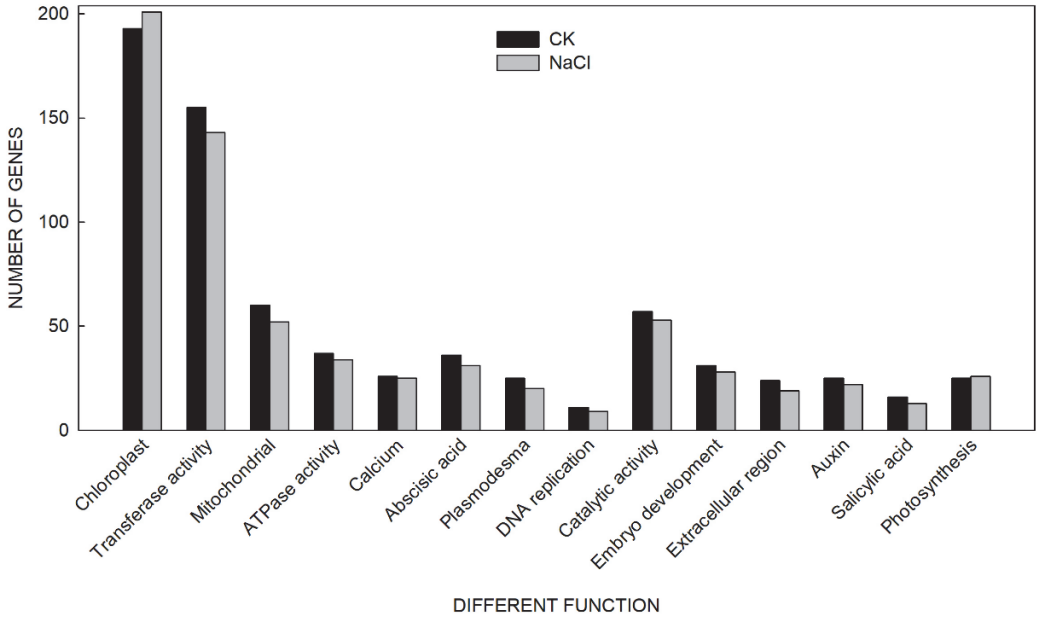

Fig. 6. The numbers of differentially expressed genes (DEGs) which in different function effected by NaCl.

Na^+ was transported to the expanded and expanding leaves (Fig. 2). Therefore, the salt tolerance mechanism of the seedlings consisted of salt exclusion under a low NaCl concentration, but the salt exclusion ability was lost under high NaCl concentrations.

With the accumulation of ions, the photosynthetic capacity of *E. angustifolia* seedlings declined. These results suggested that the effects on the photosynthetic capacity in *E. angustifolia* seedlings were dependent on the NaCl concentration. Low concentrations of NaCl (75 mM NaCl) had no impact on this parameters, but high concentrations (150–300 mM NaCl) caused significant decreases (Figs. 3, 4).

Chl is an important photosynthetic pigment in the chloroplasts of plants and performs the essential role of harvesting light energy in antenna systems and driving electron transfer in reaction centers (Green *et al*. 1991). Chl is involved in plant photosynthesis and other essential functions. Chl fluorescence is commonly employed as an indicator of stress effects, since fluorescence is highly sensitive and can be detected quickly. Seven DEGs, which were downregulated in the NaCl-treated plants were mapped to the Chl metabolism pathway. In the Chl metabolism pathway, protoporphyrinogen oxidase, magnesium chelatase, and protochlorophyllide reductase are enzymes involved in the synthesis of Chl that take part

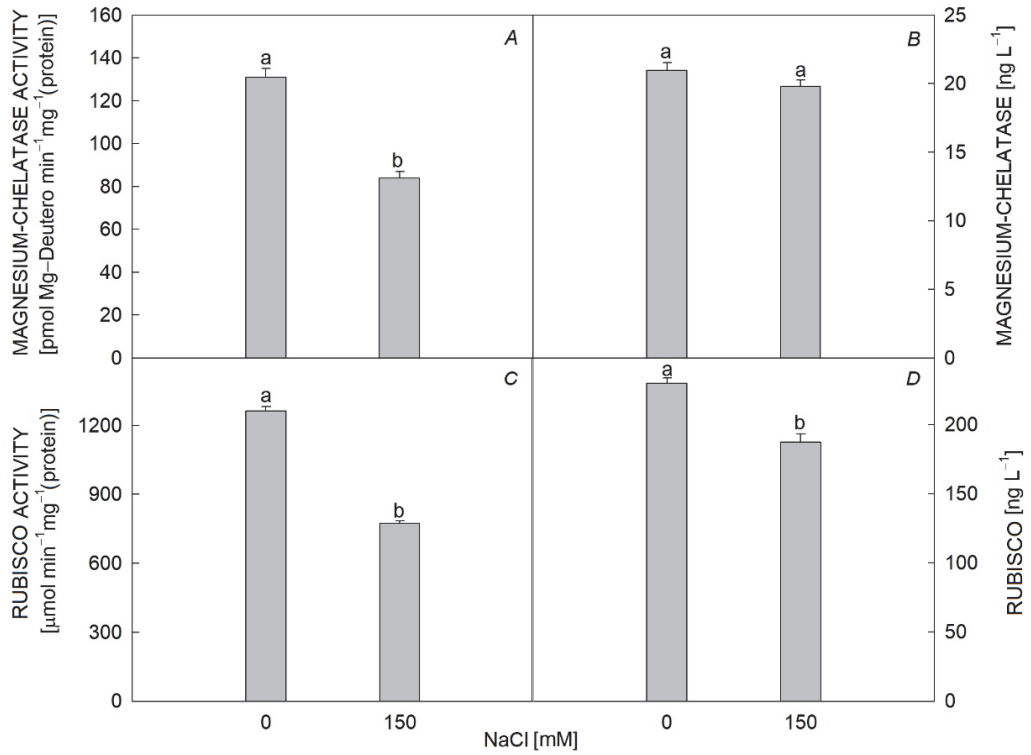

Fig. 7. The protein content and activity of magnesium-chelatase (*A*,*B*) and Rubisco (*C*,*D*) of the *Elaeagnus angustifolia* seedlings leaves under 0 and 150 mM NaCl treatment. Values are means ± SD of three replicates. Bars with the *different letters* are significantly different at $P<0.05$ according to *Duncan*'s multiple range tests.

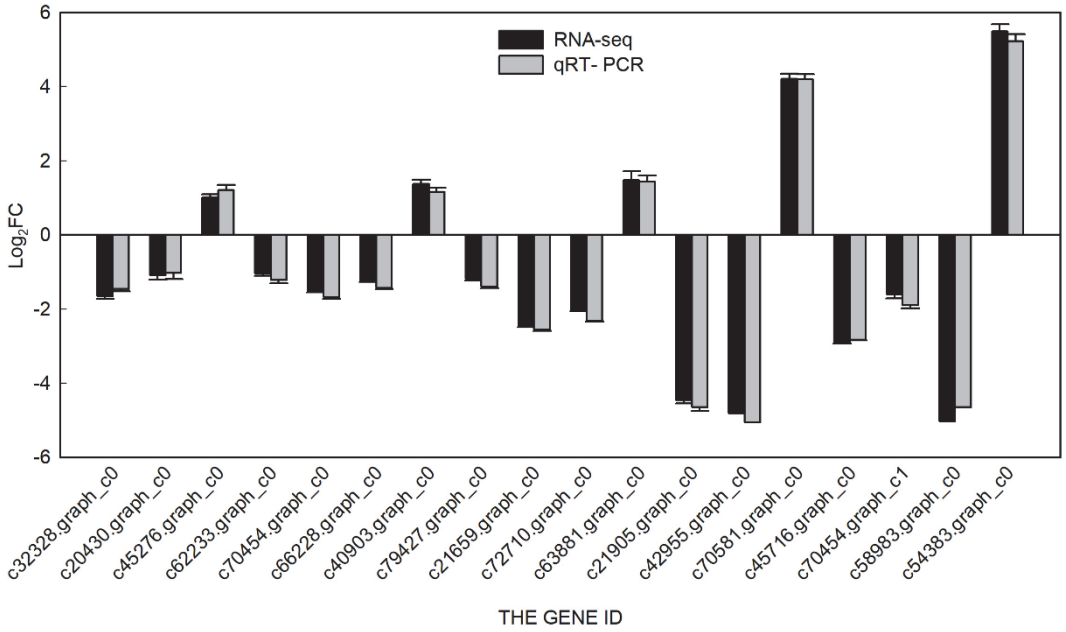

Fig. 8. Validation of RNA-Seq results by qRT-PCR. Expression levels of 18 randomly selected genes in the two samples used in this study were tested by qRT-PCR. The number in the scale bar stand for reads per KB per million (RPKM) values in RNA-Seq and ΔΔCt in qRT-PCR.

in key catalytic reactions involving protoporphyrinogen IX, protoporphyrin IX, Mg-protoporphyrin IX, and the conversion of divinyl-protochlorophyllide to divinyl-chlorophyllide (Zhang *et al*. 2006, Brzezowki *et al*. 2016) and magnesium chelatase is the key enzyme (Brzezowki *et al*. 2016). The activity and content of this enzyme were therefore measured to determine whether downregulation of the corresponding gene affected the enzyme. Our results showed that the activity of magnesium chelatase in the leaves of the seedlings was severely inhibited, while no change in the protein content was observed (Fig. 7*A*). Taking our physiological experimental results together suggested that the reduction of Chl contents in the leaves due to the NaCl treatment may be caused by down-regulation of the genes encoding key enzymes and the decrease in the activity of enzymes involved in Chl synthesis.

Under high concentration of NaCl, g_s decreased, which was accompanied by a decrease in P_N, but the decrease in the g_s largely outweighed that of C_i, indicating that the photoreaction and carbon assimilation were severely affected (Flowers and Colmer 2015). Eight DEGs mapped to light-harvesting proteins were downregulated under salt stress, suggesting that the absorption, transfer, and distribution of light energy might be inhibited under salt stress. Eight DEGs mapped to the photosynthesis pathway were also downregulated under NaCl stress, which may affect electron transport, resulting in decreased ATP and NADPH amounts in plants under NaCl stress.

Rubisco, PEPC, and PPDK are key enzymes in the dark reactions of photosynthesis. Rubisco plays an important role in CO_2 assimilation (Anderson 1971). Salt stress led to altered expression of a gene encoding Rubisco in the species, suggesting that salt stress altered the efficiency of CO_2 assimilation. To our surprise, the expression of one DEG encoding Rubisco decreased, while another DEG encoding Rubisco increased markedly after 48 h of salt stress. Rubisco is important because it catalyzes the incorporation of CO_2 into ribulose-1,5-bisphosphate, and any change in Rubisco activity has important effects on the dark reactions (Flexas *et al*. 2006). Our results showed that the protein content and enzyme activity of Rubisco significantly decreased under high NaCl concentrations (Fig. 7*B*). Taken together, our experimental results suggested that decreased CO_2 assimilation due to NaCl treatment may be caused by downregulation of the key gene encoding Rubisco, resulting in a decreased enzyme activity and protein content of Rubisco.

The other enzymes involved in the dark reactions detected in our RNA-Seq data were fructose-1,6-bisphosphatase, triosephosphate isomerase, malate dehydrogenase, and ribose-5-phosphate isomerase; the expression of the genes encoding these enzymes decreased under salt stress. Fructose-1,6-bisphosphatase converts fructose-1,6-bisphosphate into fructose-6-phosphate in the Calvin cycle (Xiao *et al*. 2014). Triosephosphate isomerase catalyzes the reversible interconversion of the triose phosphate isomers dihydroxyacetone phosphate and D-glyceraldehyde-3-phosphate (Knowles and Albery 2002). Malate dehydrogenase catalyzes the oxidation of malate to oxaloacetate, and ribose-5-phosphate isomerase catalyzes the conversion of ribose-5-phosphate to ribulose-5-phosphate (Anderson 1971). The downregulation of the expression of these genes may decrease the photosynthetic dark reactions under salt stress.

Conclusion: All the results showed that high salt concentration inhibited growth and photosynthesis of *E. angustifolia*, which was caused by the downregulation of genes encoding key enzymes involved in photosynthetic and genes related to important structures in the photosystems and light-harvesting complexes.

References

Ahmadiani A., Hosseiny J., Semnanian S. *et al*.: Antinociceptive and anti-inflammatory effects of *Elaeagnus angustifolia* fruit extract. – J. Ethnopharmacol. **72**: 287-292, 2000.

Alshammary S.F., Qian Y.L., Wallner S.J.: Growth response of four turfgrass species to salinity. – Agr. Water Manage. **66**: 97-111, 2004.

Amezketa E.: An integrated methodology for assessing soil salinization, a pre-condition for land desertification. – J. Arid Environ. **67**: 594-606, 2006.

Anderson L.E.: Chloroplast and cytoplasmic enzymes. 3. Pea leaf ribose-5-phosphate isomerases. – BBA-Enzymology **235**: 245-249, 1971.

Arnon D.I.: Copper enzymes in isolated chloroplasts, polyphenoloxidase in *Beta vulgaris*. – Plant Physiol. **24**: 1-15, 1949.

Ashburner B.M., Ball C.A., Blake J.A. *et al*.: Gene ontology: tool for the unification of biology. – Nat Genet. **25**: 25-29, 2000.

Bazakos C., Manioudaki M.E., Therios I. *et al*.: Comparative transcriptome analysis of two olive cultivars in response to NaCl-stress. – PLoS ONE **7**: e42931, 2012.

Brzezowski P., Sharifi M.N., Dent R.M. *et al*.: Mg chelatase in chlorophyll synthesis and retrograde signaling in C*hlamydomonas reinhardtii*: CHLI 2 cannot substitute for CHLI 1. – J. Exp. Bot. **67**: 3925-3938, 2016.

Chen J.B., Zhang F.R., Huang D.R. *et al*.: Transcriptome analysis of transcription factors in two melon (*Cucumis melo* L.) cultivars under salt stress. – J. Plant Physiol. **50**: 150-158, 2014.

Conesa A., Götz S., García-Gómez J.M. *et al*.: Blast2GO: a universal tool for annotation, visualization and analysis in functional genomics research. – Bioinformatics **21**: 3674-6, 2005.

Curtis P.S., Läuchli A.: The role of leaf area development and

photosynthetic capacity in determining growth of kenaf under moderate salt stress. – Funct. Plant Biol. **13**: 553-565., 1986.

Deinlein U., Stephan A.B., Horie T. *et al*.: Plant salt-tolerance mechanisms. – Trends Plant Sci. **19**: 371-379, 2014.

Feki K., Quintero J., Khoudi H. *et al*.: A constitutively active form of a durum wheat Na^+/H^+ antiporter SOS1 confers high salt tolerance to transgenic *Arabidopsis*. – Plant Cell Rep. **33**: 277-288, 2014.

Flexas J., Ribas-Carbó M.., Bota J. *et al*.: Decreased Rubisco activity during water stress is not induced by decreased relative water content but related to conditions of low stomatal conductance and chloroplast CO_2 concentration. – New Phytol. **172**: 73-82, 2006.

Flowers T.J., Colmer T.D.: Plant salt tolerance: adaptation in halophytes. – Ann. Bot.-London **115**: 327-331, 2015.

Green B.R., Pichersky E., Kloppstech K.: Chlorophyll *a/b*-binding proteins: an extended family. – Trends Biochem. Sci. **16**: 181-186, 1991.

Heid C.A., Stevens J., Livak K.J. *et al*.: Real time quantitative PCR. – Genome Res. **6**: 986-994, 1996.

Kalaitzis P., Bazakos C., Manioudaki M.: Comparative transcriptome analysis of two olive cultivars in response to NaCl stress. – PLoS ONE **7**: e42931, 2012.

Kanehisa M., Goto S., Kawashima S. *et al*.: The KEGG resource for deciphering the genome. – Nucleic Acids Res. **32**: D277-D280, 2004.

Kerkeb L., Donaire J.P., Rodríguez-Rosales M.P.: Plasma membrane H^+-ATPase activity is involved in adaptation of tomato calli to NaCl. – Physiol. Plantarum **111**: 483-490, 2001.

Khavari-Nejad R.A., Mostofi Y.: Effects of NaCl on photosynthetic pigments, saccharides and chloroplast ultrastructure in leaves of tomato cultivars. – Photosynthetica **35**: 151-154, 1998.

Khodarahmpour Z.: Effects of NaCl salinity on maize (*Zea mays* L.) at germination and early seedling stage. – Afr. J. Biotechnol. **11**: 298-304, 2001.

Knowles J.R., Albery W.J.: Perfection in enzyme catalysis: the energetics of triosephosphate isomerase. – Accounts Chem. Res. **10**: 105-111, 1977.

Liu X.X., Qi M.Y., Gao Q.J. *et al*.: [Effects of Na_2SO_4 stress on net photosynthesis rate and other physiological indexes of *Elaeagnus Mooraroftii*.] – Xinjiang Agr. Sci. **42**: 102-106, 2005. [In Chinese]

Liu Z.X., Zhang H.X., Yang X.Y. *et al*.: Effects of Na_2SO_4 stress on growth and photosynthetic physiology of *Elaeagnus angustifolia* seedlings. – For. Res. **27**: 186-194, 2014.

Livak K.J., Schmittgen T.D.: Analysis of relative gene expression data using real-time quantitative PCR and the 2-ΔΔCT method. – Methods **25**: 402-408, 2001.

Munns R., Tester M.: Mechanisms of salinity tolerance. – Annu. Rev. Plant Biol. **59**: 651-681, 2008.

Pagano E., Maddonni G.A.: Intra-specific competition in maize: Early established hierarchies differ in plant growth and biomass partitioning to the ear around silking. – Field Crop. Res. **101**: 306-320, 2007.

Song J., Ding X., Feng G. *et al*.: Nutritional and osmotic roles of nitrate in a euhalophyte and a xerophyte in saline conditions. – New Phytol. **171**: 357-366, 2006.

Sui N., Yang Z., Liu M.L., Wang B.: Identification and transcriptomic profiling of genes involved in increasing sugar content during salt stress in sweet sorghum leaves. – BMC Genomics **16**: 2-18, 2015.

Sun W., Xu X., Zhu H. *et al*.: Comparative transcriptomic profiling of a salt-tolerant wild tomato species and a salt-sensitive tomato cultivar. – Plant Cell Physiol. **51**: 997-1006, 2010.

van Kooten O., Snel J.F.: The use of chlorophyll fluorescence nomenclature in plant stress physiology. – Photosynth. Res. **25**: 147-50, 1990.

Whitney S.M., Houtz R.L., Alonso H.: Advancing our understanding and capacity to engineer nature's CO_2-sequestering enzyme, Rubisco. – Plant Physiol. **155**: 27-35, 2011.

Xiao H.D., Chen C.S., Xu Y. *et al*.: Cloning and expression analysis of the chloroplast fructose-1,6-bisphosphatase gene from *Pyropia haitanensis*. – Acta Oceanol. Sin. **33**: 92-100, 2014.

Zhang H., Li Z., Yoo J.H. *et al*.: Rice Chlorina-1 and Chlorina-9 encode Chl D and Chl L subunits of Mg-chelatase, a key enzyme for chlorophyll synthesis and chloroplast development. – Plant Mol. Biol. **62**: 325-337, 2006.

Zhao K., Fan H., Zhou S., Song J.: Study on the salt and drought tolerance of *Suaeda salsa* and *Kalanchoe claigremontiana* under iso-osmotic salt and water stress. – Plant Sci. **165**: 837-844, 2003.

Zhu J.K.: Plant salt tolerance. – Trends Plant Sci. **6**: 66-71, 2001.